


# A comparison of 2D and 3D numerical simulations of tunnelling in soft soils

Ngoc Anh Do<sup>1</sup> · Daniel Dias<sup>2</sup> 

Received: 27 September 2016 / Accepted: 16 January 2017 / Published online: 24 January 2017  
© Springer-Verlag Berlin Heidelberg 2017

**Abstract** Tunnel excavation is a three-dimensional problem, especially in the zone close to the tunnel face. However, despite recent advances in computing resources, a full 3D numerical analysis is usually complex and requires important computational resources (both in terms of storage and of time). Two-dimensional simulations are therefore often used. In this paper, the Hanoi metro system is used as a case study. A numerical investigation is performed to evaluate the applicability of 2D deconfinement methods. These methods consider pre-displacements of the soil surrounding the tunnel before installation of the tunnel structure to model the 3D phenomenon which occurs at the tunnel face. The obtained results allow estimating the 2D deconfinement method which gives the better agreement with the 3D model in terms of both soil movements and structural forces induced in the tunnel lining using an error function. These estimations were performed at different sections along the tunnel direction in order to highlight the effect of the tunnel advancement on the applicability of 2D deconfinement methods.

**Keywords** Tunnelling · Soft soil · Numerical calculations

## Introduction

Tunnel excavation is a three-dimensional (3D) problem, especially in the zone close to tunnel face (Arnau and Molins 2012; Mollon et al. 2013; Do et al. 2015). However, despite recent advances in computing resources, 3D numerical models are still not frequently used due to calculation time and complexity, and two-dimensional (2D) simulations are therefore often used for its reduced calculation time and relative simplicity (Muniz de Farias et al. 2004; Negro and Queiroz 2000; Do et al. 2013; Callari and Casini 2005; Cattoni et al. 2016).

After excavation, the stress–strain state in the soil surrounding the tunnel is modified and necessitates to reach a new equilibrium. At this new equilibrium, displacements of the soil and structural forces developed in the tunnel lining strongly depend on the moment of support structure installation and on its stiffness. The pre-displacements of the surrounding soil before installing the support structure are hereafter called deconfinement or relaxation process (Do et al. 2014a). This process is considered in 3D numerical models. However, it is necessary to use some specified methods to take into account this process in 2D numerical models.

The available methods that allow the deconfinement process to be considered include: the convergence confinement method (CCM) (Panet and Guenot 1982; Hejazi et al. 2008; Janin et al. 2015), the gap method (Cattoni et al. 2016; Rowe et al. 1983; Tamagnini et al. 2005), the progressive softening method (Swoboda 1979), the contraction method (Vermeer and Brinkgreve 1993), the volume loss control method (VLM) (Hejazi et al. 2008; Addenbrooke et al. 1997; Jenck and Dias 2004; Wongsaraj et al. 2013), the grout pressure method (Möller and Vermeer 2008) and the modified grout pressure method (Surrarak 2010).

---

✉ Daniel Dias  
daniel.dias@univ-grenoble-alpes.fr

<sup>1</sup> Department of Underground and Mining Construction, Faculty of Civil Engineering, Hanoi University of Mining and Geology, Hanoi, Vietnam

<sup>2</sup> Laboratory 3SR, Grenoble Alpes University, Grenoble, France

Tamagnini et al. (2005) and Cattoni et al. (2016) performed 2D tunnelling simulations by imposing a non-uniform gap closure which allows to take into account of the volume loss effects and of the tunnel ovalization. Using a parametric study for two different case-histories of tunnelling in soft clays, their results pointed out the importance of the tunnel ovalization on the predicted displacement field.

Karakus (2007) used various 2D numerical simulations and compared obtained results with the settlement profile in the transverse section monitored during the construction of the Heathrow Express tunnel in London. The best fit with the in situ measurements is obtained with the convergence confinement method (Panet and Guenot 1982). This method was also verified by Svoboda and Mašín (2009) who compared displacement field obtained by 2D and 3D finite element models of shallow tunnels in clays. Their results pointed out that for an optimum value of stress relaxation ratio in the CCM method, the predicted displacement determined by 2D simulation agreed well with the 3D model. Callari and Casini (2005) presented two and three-dimensional studies in saturated poro-elasto-plastic soils in order to estimate the CCM method effectiveness. Using a hydro-mechanically coupled formulation, they investigated the face advance rate influence on the soil response to excavation. The proposed 2D method showed to be able to reproduce with accuracy the effects of the tunnel face advancement. It should be mentioned that in most of the cases reported in the literature used only the surface settlements as a criterion to compare 2D with 3D numerical models.

The work conducted by Janin et al. (2015) was more complete and indicated that the settlement profile determined with means of the CCM method, using a couple of stress relaxation ratios which allow the influence of the multi-phase construction to be taken into account, was in good agreement with both 3D numerical results and measured data.

In reality, besides soil movements, structural forces induced in the tunnel lining are also important parameters which need to be taken into account during tunnelling. Möller and Vermeer (2008) simulated the excavation of a tunnel in Stuttgart. On the basis of the settlement that develops on the soil surface and the structural forces induced in a continuous lining, they concluded that it is necessary to use two different stress release values ( $\lambda_d$ ) depending whether it is desired to estimate soil settlements or stresses in the support. They also proposed the grout pressure method and evaluated its merits by comparing it with the CCM method and VLM method. By comparing 2D and 3D numerical results applied to a mechanized tunnelling in urban area, Do et al. (2014a) highlighted the influence of the CCM method and VLM method on the

behavior of tunnel in terms of both soil movements and structural forces developed in the tunnel lining. Their results indicated that the structural forces obtained by the CCM method are in better agreement with the 3D numerical results than the ones determined with the VLM method. It should be noted that the applicability of the deconfinement or the relaxation processes in the works conducted by Möller and Vermeer (2008) and Do et al. (2014a) were estimated at the steady state far from the tunnel face. Their applicability at sections close to the tunnel face is still a question.

In this paper, a numerical investigation is performed using the FLAC<sup>3D</sup> software (Itasca Consulting Group 2009) to evaluate the applicability of CCM and VLM methods at different sections along the tunnelling direction. The obtained results allow estimating the 2D method which gives the better agreement with the 3D model in terms of both soil movements and structural forces induced in the tunnel lining using an error function.

## Numerical simulation

The parameters from the Nhon-Hanoi Railway station section of the Hanoi pilot light underground in Vietnam were adopted in this study (Hanoi Metropolitan Railway Management Board (MRB) 2012). This is a 12.5-km-long twin tunnels which are excavated close to each other (1.54 D of distance) and still under construction. The external excavation diameter (D) of the tunnel is 6.3 m. A typical cross section is chosen in this study (see Fig. 1).

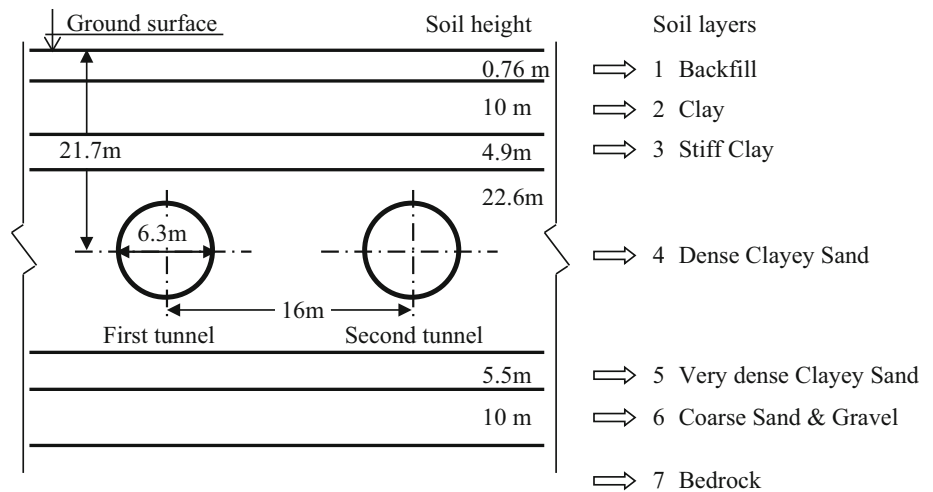
A study conducted by Do et al. (2014b) indicated that the critical influence distance between two tunnels is about two tunnel diameters. Therefore, for the sake of simplicity, all calculations performed in this study considering only the excavation of a single first tunnel without paying attention to the presence of the second tunnel.

## Behavior of the soils

Depending on the characteristics of the soil layers, two constitutive models were adopted in the 2D and the 3D numerical models. While the linear elastic perfectly plastic constitutive model with a Mohr–Coulomb failure criteria (named MC) is used for clayey soil (layers 1, 2, 3 and layer 7) due to a lack of geotechnical tests, the CYsoil (Itasca Consulting Group 2009) constitutive model is applied for sandy layers 4, 5 and 6.

The CYsoil model is a strain-hardening constitutive model that is characterized by a frictional Mohr–Coulomb shear envelope and an elliptic volumetric cap in the ( $p'$ ,  $q$ ) plane. In the CYsoil model, the stiffness is adopted as a function of the effective confinement and it leads to a

**Fig. 1** Geological conditions of the considered section (not scaled)



higher value for the unloading–reloading stiffness. If a friction hardening behavior is adopted, the input parameters are (Itasca Consulting Group 2009):

- Elastic tangent shear modulus  $G_{ref}^c$  at reference effective pressure  $p^{ref}$  (equal to 100 kPa) ( $G_{ref}^c = E / (2(1 + \nu))$ );
- Failure ratio  $R_f$  which is a constant and smaller than 1 (0.9 in most cases);
- Ultimate friction angle  $\phi_f$ ;
- Calibration factor  $\beta$ .

Geotechnical properties of the soil layers are provided in Table 1.

**2D numerical simulation**

A plane strain configuration is used in the 2D models, and the initial stress state is calculated under the gravity effect.

*Tunnel lining*

Segmental concrete lining for a tunnelling boring machine generally comprises a sequence of rings. In this studied case, each tunnel ring is made up of six uniform segments, corresponding to six segment joints, which are assumed located at angles of 0°, 60°, 120°, 180°, 240° and 300°, measured counter-clockwise from the spring line on the right. The parameters of the tunnel lining were assumed as follows: Young’s modulus  $E_1 = 35.000$  MPa; Poisson’s ratio  $\nu_1 = 0.15$ ; thickness  $A_1 = 0.3$  m. The tunnel lining was modeled using embedded liner elements (Do et al. 2013). Embedded liner elements and soil surrounding the tunnel are attached together through the presence normal stiffness  $k_n$  and tangential stiffness  $k_s$  (Itasca Consulting Group 2009).

The segment joints were simulated using double node connections. Each node connection is represented by six springs: three translational components in the  $x$ ,  $y$  and  $z$  directions, and three rotational components around the  $x$ ,  $y$  and  $z$  directions. In this study, the stiffness characteristics of the joint connection are represented by a set composed of a rotational spring ( $K_\theta$ ), an axial spring ( $K_A$ ) and a radial spring ( $K_R$ ) (Do et al. 2013). While the behavior of the axial springs ( $K_A$ ) was represented by a linear relation using a constant coefficient spring, both the rotational stiffness ( $K_\theta$ ) and the radial stiffness ( $K_R$ ) of a segment joint were modeled, by means of a bilinear relation (Do et al. 2013). The segment joint parameters are presented in Table 2.

*Tunnelling simulation*

In order to estimate the applicability of the available 2D simulation methods, the deconfinement process induced in the soil surrounding the tunnel before installing the support structure is performed using the CCM method and VLM method. These simplified methods were introduced to simulate the 3D tunnelling process. They do not permit to take into account all the complexity of the excavation processes but are commonly used in geotechnical engineering.

In the case of using the CCM method, numerical simulation is done as the following phases:

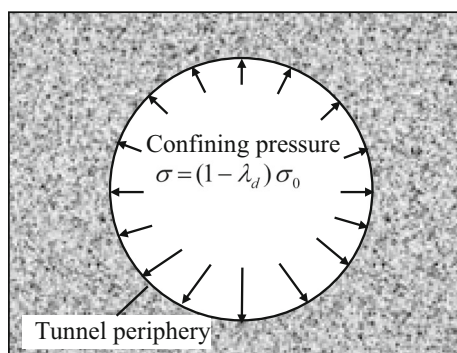
- Deactivating the soil inside the tunnel and simultaneously applying radial pressures to the tunnel circumference and toward the soil medium (see Fig. 2). The value of the radial pressure is determined using Eq. (1), which depends on in situ stress existing inside the soil and is not constant around the tunnel boundary.

**Table 1** Geomechanical properties

Properties/ground layers	Layer 1	Layer 2	Layer 3	Layer 4	Layer 5	Layer 6	Layer 7
Applied constitutive model	MC	MC	MC	CYsoil	CYsoil	CYsoil	MC
Thickness (m)	0.76	10	4.9	22.6	5.5	10	–
Density (kN/m <sup>3</sup> )	14	16	19	20	20	21	23
Earth pressure coefficient at rest $K_0$	0.74	0.66	0.58	0.44	0.43	0.4	0.29
Confinement pressure $\sigma_3$ (kPa)	3.9	59.8	128.4	217.3	333.2	372.3	–
<i>Mohr–Coulomb model's parameters</i>							
$E$ (Young's modulus) (MPa)	1	2.8	5.2	10	10	150	15,000
$\nu$ (Poisson's ratio)	0.42	0.39	0.37	0.31	0.3	0.28	0.35
$\phi$ (friction angle) (°)	15	20	25	34	35	37	45
$\psi$ (dilation angle) (°)	0	0	0	0	0	0	0
$c$ (cohesion) (kPa)	5	5	25	0	0	0	200
<i>CYsoil model's parameters</i>							
Elastic shear modulus $G$ (MPa)				8.3	12.8	218.1	
Elastic bulk modulus $K$ (MPa)				19.1	27.8	423.1	
Reference effective pressure $p^{\text{ref}}$ (kPa)				100	100	100	
Failure ratio $R_f$				0.9	0.9	0.9	
Ultimate friction angle $\phi_f$ (°)				34	35	37	
Calibration factor $\beta$				2.75	1.70	1.25	
Reference elastic tangent shear modulus (MPa)				3.82	3.85	58.59	

**Table 2** Parameters of the joints in the present models

Segment joints	Value	Ring joints	Value
Rotational stiffness $K_\theta$ (MN m/rad/m)	100	Rotational stiffness $K_{\theta R}$ (MN m/rad/m)	100
Maximum bending moment at segment joint $M_{\text{yield}}$ (kN m/m)	150	Maximum bending moment at ring joint $M_{R\text{yield}}$ (kN m/m)	150
Axial stiffness $K_A$ (MN/m)	500	Axial stiffness $K_{AR}$ (MN/m)	500
Radial stiffness $K_R$ (MN/m)	1050	Radial stiffness $K_{RR}$ (MN/m)	1050
Maximum shear forces at segment joint $S_{\text{yield}}$ (MN/m)	0.55	Maximum shear forces at ring joint $S_{R\text{yield}}$ (MN/m)	0.55

**Fig. 2** 2D simulation with the CCM method

$$\sigma = (1 - \lambda_d)\sigma_0 \quad (1)$$

where  $\sigma$ , radial pressure (kN/m<sup>2</sup>);  $\sigma_0$ , initial stress in the soil medium (kN/m<sup>2</sup>);  $\lambda_d$ , stress relaxation coefficient.

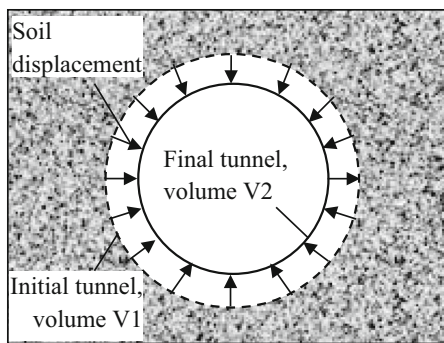
- Activating the support structure and the total relaxation ( $\lambda_d = 1$ ) is applied to nodes along the tunnel boundary.

In the case of applying the VLM methods, two different simulation techniques are used: (1) VLM method with fixed center (VLM-fix method) (Hejazi et al. 2008) and (2) VLM method with free center (VLM-free method) (Do et al. 2014a).

Using the VLM-fix method, the shape of the tunnel boundary is always circular during the deconfinement process and its center is fixed (see Fig. 3). The displacement process of the tunnel boundary is stopped when the volume loss reaches a specified value. These uniform displacements can be observed when a tunnel is excavated through a soil mass with the earth pressure coefficient at rest  $K_0$  of unity. In other cases of the  $K_0$  factor, deformed boundary of the tunnel is usually noncircular after the deconfinement process (see Fig. 4) which is considered in the VLM-free method (Do et al. 2014a).

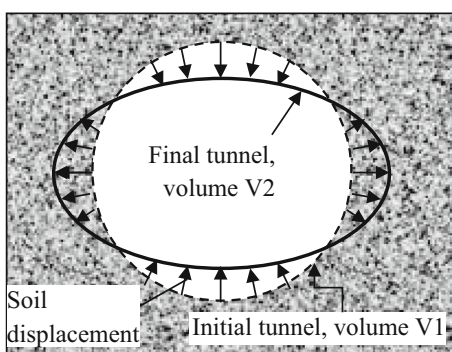
In the present study, the deconfinement process is simulated using the VLM methods in the following steps:

- Deactivating the soil inside the tunnel boundary;
- Deconfinement process:



$$\text{Volume loss } V_l = (V_1 - V_2) / V_1 * 100 (\%)$$

**Fig. 3** 2D simulation with the VLM-fix method (fixed tunnel boundary)

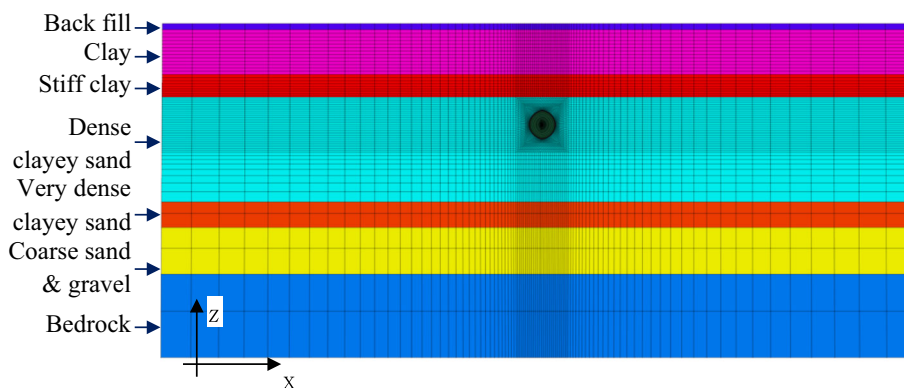


$$\text{Volume loss } V_l = (V_1 - V_2) / V_1 * 100 (\%)$$

**Fig. 4** Tunnelling simulation with the VLM-free method (free tunnel boundary)

- + In the case of using the VLM-fix method: The nodes along the tunnel boundary are radially moved with the same magnitude.
  - + In the case of using the VLM-free method: The nodes along the tunnel boundary are freely moved.
- The deformed area of the tunnel is continuously updated at each computation cycle during the displacement of the tunnel boundary;

**Fig. 5** 2D numerical model introduced into FLAC<sup>3D</sup>



- + The numerical performance is stopped when the volume loss value determined using the formula presented in Figs. 3 and 4 reaches a specified value;
- Activating the support structure.

Figure 5 presents the plane strain model grid. The elements dimension increases as one moves away from the tunnel. The numerical model is 184 m wide in the x-direction, 72 m high in the z-direction and consists of approximately 14,260 zones and 28,712 grid points. The same model grid was created for 2D and 3D simulations using Flac<sup>3D</sup>. In the 2D case, a 3D slice of 1 m was considered.

### 3D numerical simulation

The objective of 3D numerical analysis is to estimate the applicability of the 2D deconfinement methods. The tunnel construction process is modeled using a step-by-step approach (Mollon et al. 2013; Jenck and Dias 2004; Do et al. 2014c, d, e). The advance length of 1.5 m after each excavation which is equal to the width of a lining ring installed at the shield tail is used.

In this 3D numerical model, most components of a mechanized tunnelling using shield machine were simulated: trapezoidal distribution pressure applied from the chamber behind the tunnel face, distribution pressure applied to the soil surface in the cylindrical void just behind the tunnel facet, the shield and its conicity, the self-weight of the shield machine, the jacking force applied on the lining ring at the shield tail, the grouting pressure behind the shield tail and the hardened grout, the tunnel linings with the joints and the back-up train. Detailed descriptions of each of the above components can be seen in the work by the same authors (Do et al. 2014c, d, e, f), and these are therefore not described here again.

The presence of the joints in the tunnel lining is taken into consideration in this 3D model. Beside longitudinal joints between segments in a ring as described in 2D



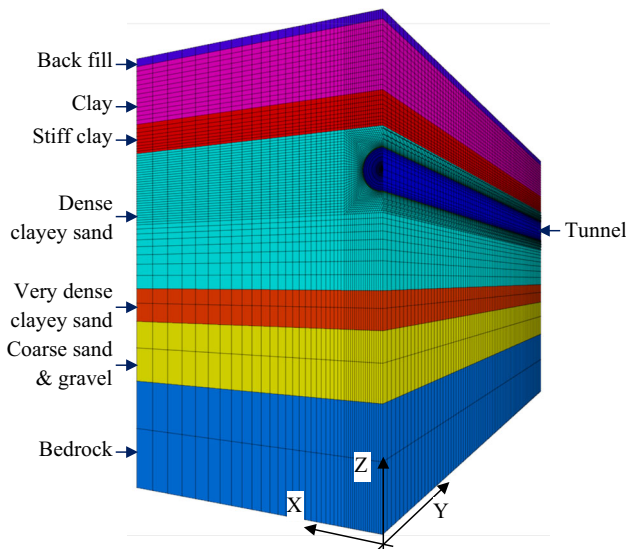


**Fig. 6** Half of perspective 3D numerical model introduced into FLAC<sup>3D</sup>

models, circumferential joints between successive rings also considered which are simulated by a set composed of a rotational spring ( $K_{\theta R}$ ), an axial spring ( $K_{AR}$ ) and a radial spring ( $K_{RR}$ ) (Do et al. 2014f). Parameters of the ring joints are summarized in Table 2.

The 3D model grid (Fig. 6) is the same as the one presented at Fig. 5 in the X–Z plane, and 120 m length in the y-direction is considered. This model consists of approximately 1,114,240 zones and 1,135,620 grid points.

### Numerical results and discussion

In order to estimate the better 2D deconfinement method giving the results which are closest to those obtained using 3D numerical model, an error function presented in Eq. (2) was adopted. This error function considered the settlement parameters (maximum settlement “ $S_{max}$ ” and distance from the central line of the tunnel to the

inflection point of the settlement trough “ $i$ ”) based on the Peck’s formula (Panet and Guenot 1982), the horizontal movement ( $X_{top}$ ) of point A at the soil surface, the horizontal movement ( $X_{tunnel}$ ) of point B on the spring line of the tunnel which are at a distance of 1D from the vertical axis of the tunnel (see Fig. 7) and the internal forces in the lining (bending moment and normal force). Due to the fact that mechanized tunnelling is a 3D process, soil movements are not the same along the tunnelling direction. For this reason, above parameters were determined at some typical transverse sections in the 3D model that is at the shield tail, at  $1 L_S$  (the length from cutter head to the end shield tail), at  $2 L_S$  and at  $5 L_S$  behind the shield tail at which the tunnel behavior reaches a steady state. The expression of the error function is given in Eq. (2) which is used to calculate the error function at each of the above transverse sections.

$$f(S, i, X, M, N) = \left( \frac{S_{2D} - S_{3D}}{S_{3D}} \right)^2 + \left( \frac{i_{2D} - i_{3D}}{i_{3D}} \right)^2 + \left( \frac{X_{2D} - X_{3D}}{X_{3D}} \right)^2 + \left( \frac{M_{2D} - M_{3D}}{M_{3D}} \right)^2 + \left( \frac{N_{2D} - N_{3D}}{N_{3D}} \right)^2 \tag{2}$$

where  $S_{2D}$ ,  $S_{3D}$ : maximum settlements obtained, respectively, with the 2D model and the 3D model;  $i_{2D}$ ,  $i_{3D}$ : distances from inflection point of settlement trough to the center line obtained, respectively, with the 2D model and the 3D model;  $X_{2D}$ ,  $X_{3D}$ : horizontal movements of point A (or B) (see Fig. 7) obtained, respectively, with the 2D model and the 3D model;  $M_{2D}$ ,  $M_{3D}$ : maximum bending moments induced in the tunnel lining obtained, respectively, with the 2D model and the 3D model;  $N_{2D}$ ,  $N_{3D}$ : maximum normal forces induced in the tunnel lining obtained, respectively, with the 2D model and the 3D model.

In 2D simulations using deconfinement methods, it is always difficult to choose relaxation factor ( $\lambda_d$ ) or volume loss ratios (VL) in the CCM method and VLM methods, respectively. These values have a major impact on the

**Fig. 7** Observed parameters of the soil movement

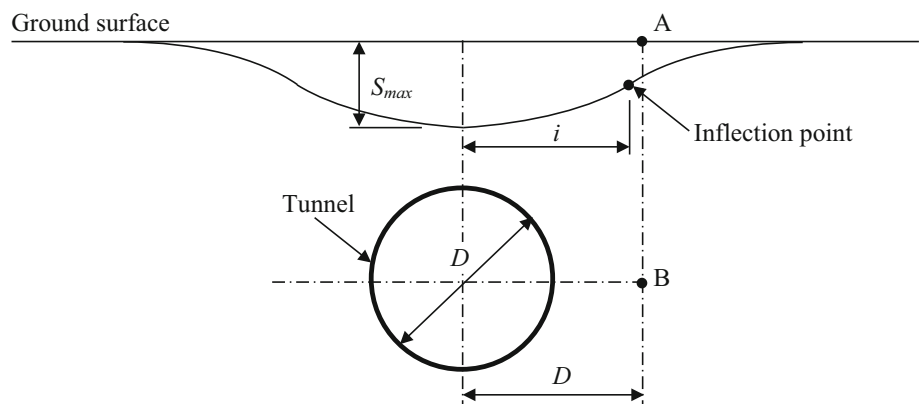


**Table 3** Optimization criterion for different scenarios

Section	Simplified method	Scenario 1	Scenario 2	Scenario 3	Scenario 4
Shield tail	VLM-free	<b>0.40% (0.00)</b>	0.50% (0.105)	<b>0.45% (0.378)</b>	<b>0.50% (0.488)</b>
	VLM-fix	1.25% (0.001)	<b>1.25% (0.004)</b>	1.25% (0.631)	1.25% (0.633)
	CCM	0.10 (0.001)	0.125 (0.041)	0.10 (0.63)	0.10 (0.522)
1 $L_S$ (12 m)	VLM-free	0.90% (0.00)	0.90% (0.021)	<b>0.90% (0.316)</b>	<b>0.90% (0.337)</b>
	VLM-fix	1.85% (0.00)	1.85% (0.012)	1.75% (0.594)	1.75% (0.593)
	CCM	0.20 (0.00)	<b>0.20 (0.00)</b>	0.185 (0.430)	0.185 (0.430)
2 $L_S$ (24 m)	VLM-free	<b>1.05% (0.00)</b>	1.05% (0.01)	<b>1.05% (0.30)</b>	<b>1.05% (0.31)</b>
	VLM-fix	2.0% (0.001)	2.0% (0.02)	1.85% (0.576)	1.85% (0.596)
	CCM	0.225 (0.002)	<b>0.225 (0.003)</b>	0.2 (0.419)	0.2 (0.419)
5 $L_S$ Final state	VLM-free	1.05% (0.00)	1.05% (0.09)	<b>1.05% (0.295)</b>	<b>1.05% (0.304)</b>
	VLM-fix	2.0% (0.00)	1.95% (0.02)	1.85% (0.573)	1.85% (0.591)
	CCM	0.225 (0.00)	<b>0.225 (0.003)</b>	0.2 (0.417)	0.2 (0.417)

Bold values indicate correspond to the case of the smaller error function value for each scenario and for each tunnel section

VLM-free: volume loss method using free center technique; VLM-fix: volume loss method using fixed center technique; CCM: convergence confinement method; a% (b): a and b represent the volume loss ratio in VLM methods and the error function value, respectively; c (b): c and b represent the relaxation value in CCM method and the error function value, respectively

numerical results, both in terms of soil deformation and stresses developed in the support system. Unfortunately, their values are somewhat arbitrarily chosen during the design process.

In this study, for each 2D deconfinement method, a series of calculations is conducted using different values of relaxation factor ( $\lambda_d$ ) and volume loss ratio (VL) in CCM method and VLM methods, respectively.

For each transverse section along the longitudinal axis of the tunnel in 3D numerical model, the best values of relaxation factor ( $\lambda_d$ ) and volume loss ratio (VL) in 2D deconfinement methods are determined using the error function presented at Eq. (2).

Settlement trough on the soil surface and horizontal displacements are often monitored during excavation of a mechanized tunnel in urban area. However, due to the complexity of construction process, some of them can in reality be omitted. It is therefore interesting to estimate the most appropriate deconfinement method based on different scenarios of monitored parameters as follows:

- Scenario 1: considering only the maximum settlement ( $S_{max}$ );
- Scenario 2: considering the maximum settlement ( $S_{max}$ ) and distance from inflection point ( $i$ );
- Scenario 3: considering the maximum settlement ( $S_{max}$ ), lateral movement on the soil surface ( $X_{top}$ ) and lateral movement at the tunnel center level ( $X_{tunnel}$ );
- Scenario 4: considering the maximum settlement ( $S_{max}$ ), distance from inflection point ( $i$ ), lateral movement on the soil surface ( $X_{top}$ ) and lateral movement at the tunnel center level ( $X_{tunnel}$ );

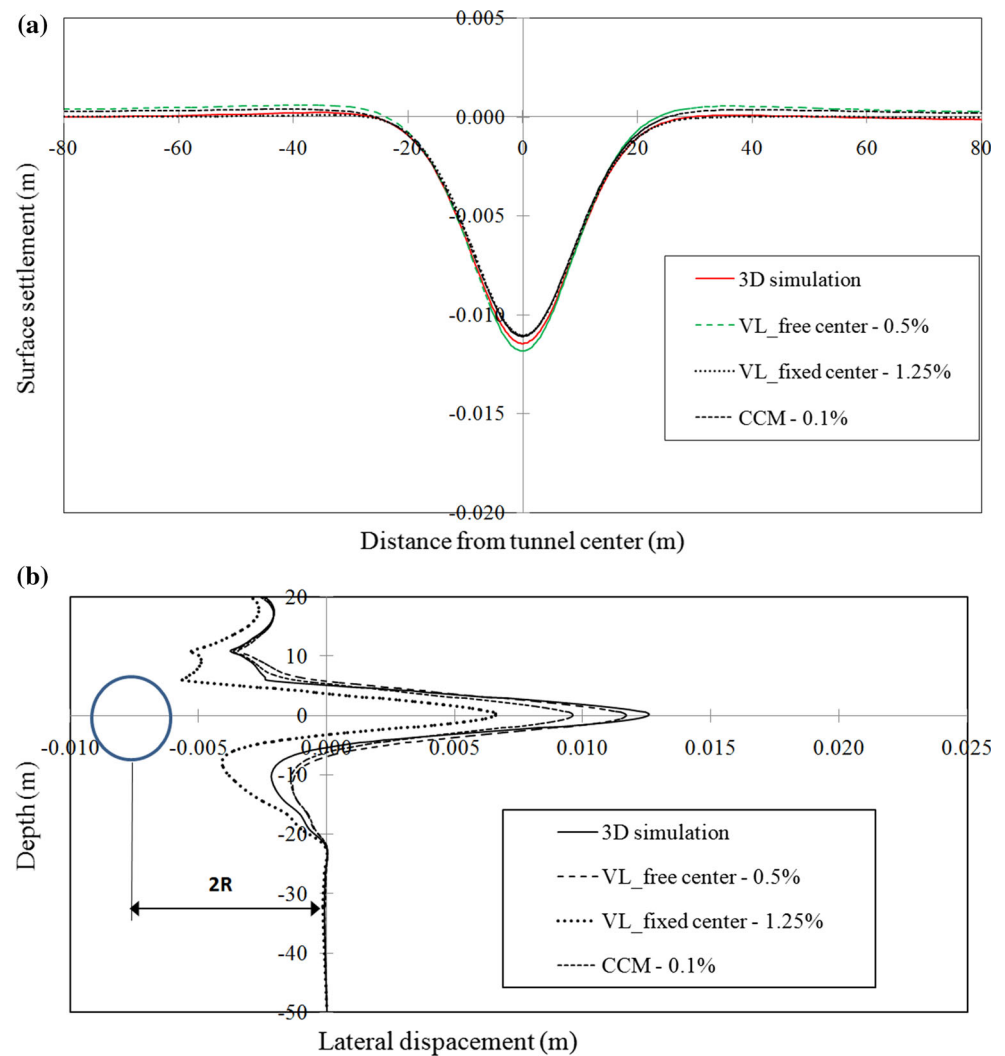
- Scenario 5: considering parameters presented in scenario 4 plus the maximum bending moment ( $M$ ) and maximum normal forces ( $N$ ) induced in the tunnel lining.

Table 3 and Figs. 8, 9 and 10 present the optimization criterion for scenarios from 1 to 4 considering different 2D deconfinement methods. With VLM-free method and VLM-fix method (Table 3), while the percentage value implies the volume loss value, the number inside the bracket means the error function value determined using Eq. (2). In the case of the CCM method, bracketed value is also the error function value obtained using Eq. (2) and the other value means the stress relaxation coefficient as mentioned in Eq. (1). The light gray cells permit to highlight the best 2D case (smallest error function value).

As given in Table 3, in the case of scenario 1 where only the maximum settlement value  $S_{max}$  is considered, all three deconfinement methods (using an appropriate deconfinement factor) can give results which are in good agreement with those obtained with the 3D model. The values of the error function are approximately null.

With scenario 2, the maximum settlement ( $S_{max}$ ) and the distance of the inflection point ( $i$ ) are adopted, and absolute values of error function and the difference between the error function values obtained from the deconfinement methods and at different transverse sections are very low, except for the shield tail section. It is, however, interesting to note that CCM method usually gives the best fitting between 2D and 3D models. This observation is in good agreement with the conclusion obtained in researches conducted by Do et al. (2014a) and Janin et al. (2015).

**Fig. 8** Surface settlements (a) and lateral displacements (b) at the shield tail section



Unlike scenarios 1 and 2, in both scenarios 3 and 4 where parameters of settlement trough and lateral movements are considered, the applicability of 2D deconfinement methods to reproduce the 3D simulation is not similar. In both scenarios 3 and 4, the VLM-free method always gives the best fitting with 3D results at different transverse sections. On the other hand, the maximum difference between results obtained from 2D and 3D models is observed in the case of using the VLM-fix method. It is also interesting to note that the best volume loss ratios adopted in 2D simulations are more or less similar in all scenarios from 1 to 4, except for the shield tail section. It is necessary to mention that the smallest values of the error function obtained in both scenarios 3 and 4 are higher than those determined in scenarios 1 and 2 (Table 3). The difference between 2D and 3D numerical models increases when considering both vertical and horizontal displacement of the surrounding soil.

The VLM-free method gives the better results compared to those calculated with a 3D model when considering both vertical settlements and lateral movements of the soil surrounding the tunnel. This conclusion is not the same as in the case of considering only the vertical settlements trough. In other words, depending on the parameters which will be monitored (e.g., vertical displacement and/or horizontal displacement), different 2D deconfinement method should be adopted.

It is important to note that the optimum value of volume loss ratio (VL) or deconfinement factor ( $\lambda_d$ ) adopted in the VLM and CCM methods, respectively, is similar in all of optimization scenarios, except for the transverse section at the shield tail. It means that one of the four above optimization scenarios can be used to estimate the optimum relaxation parameters (VL or  $\lambda_d$ ) applied in the 2D simulations without final significant differences.

All the optimized parameters: volume loss (VL) or deconfinement factor ( $\lambda_d$ ) in the VLM and CCM methods,



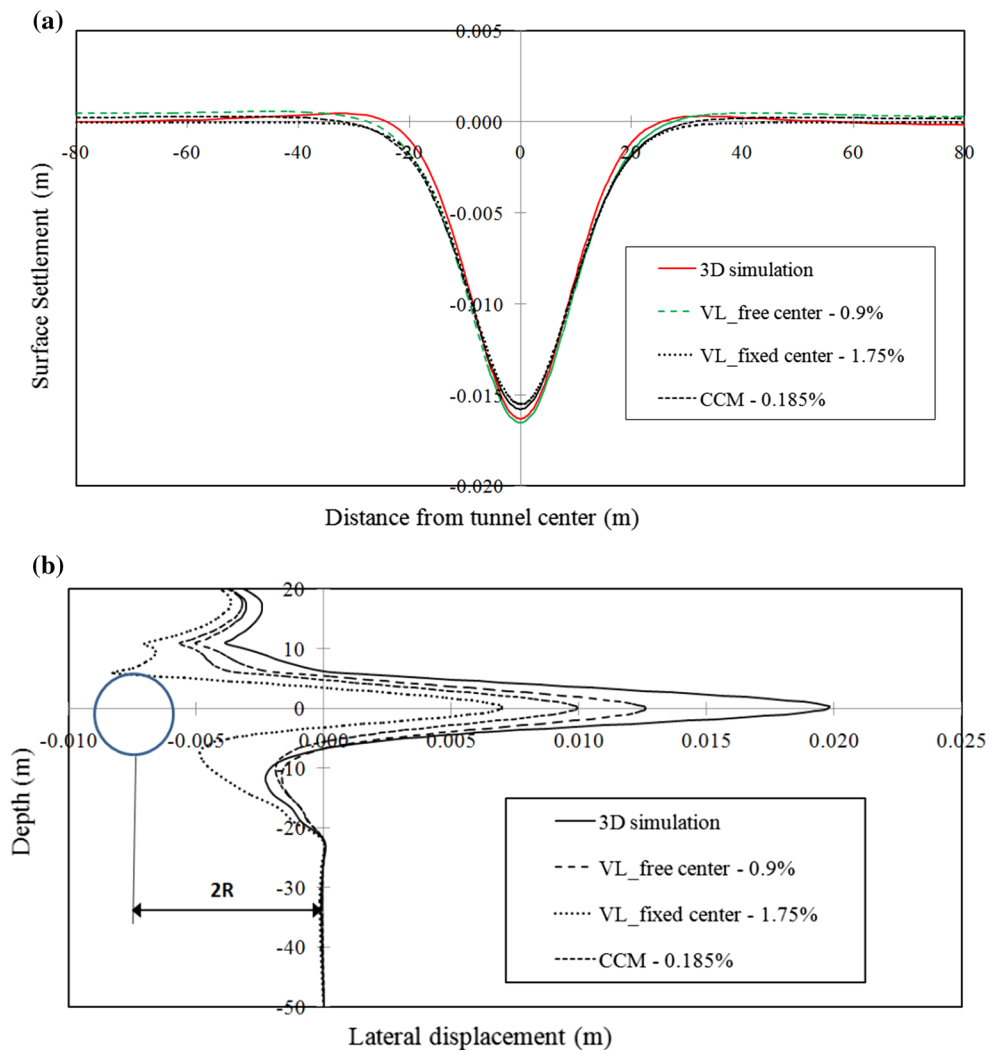


**Fig. 9** Surface settlements (a) and lateral displacements (b) at a distance  $1 L_S$  behind the shield tail

respectively, obtained at transverse sections located at a distance of  $2 L_S$  from the shield tail are similar as those obtained at the steady state. The optimized parameters (VL or  $\lambda_d$ ) determined at this steady-state section can then be used in 2D calculation of tunnels.

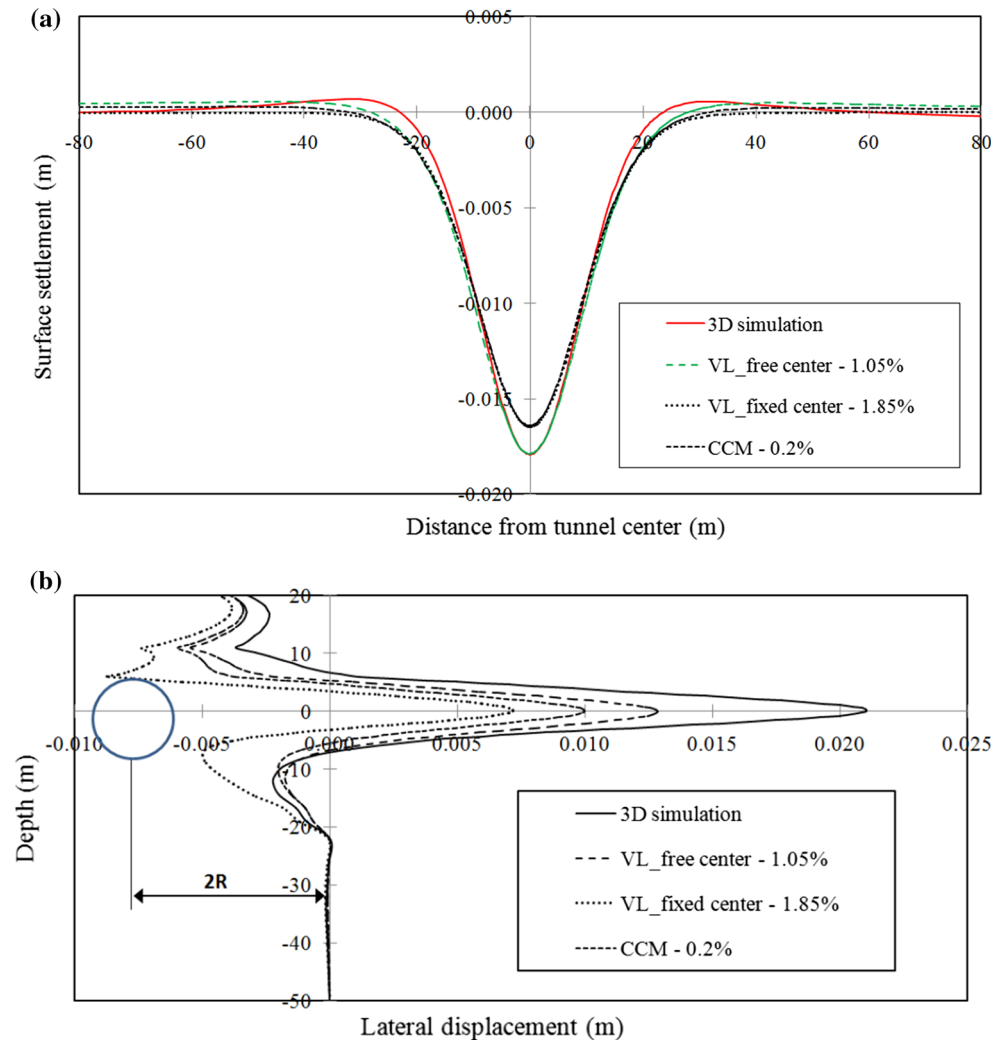
In reality, beside movements of the soil surrounding the tunnel, structural forces induced in the tunnel lining are also important parameters which should be paid attention during tunnelling. Evidently, movements of the surrounding soil have strong effect on the behavior of the tunnel lining. In the three above 2D deconfinement methods, the movements of the soil surrounding the tunnel during relaxation process are significantly different. Consequently, differences in structural forces induced in the tunnel lining observed in these 2D simulations are predicted. For the sake of simplification, only structural forces induced in the tunnel lining at the final state which is far enough behind the shield tail are considered. At this transverse section,

structural forces in the tunnel lining reach the maximum values.

With the same deconfinement parameters adopted for the best optimization in terms of settlement trough and lateral movements mentioned above, while volume loss method using free center technique gives the better agreement with the 3D model in terms of soil movements, structural forces obtained using CCM method are the most appropriate. Indeed, the CCM method gives a good fitting of the bending moment diagram not only in terms of absolute values but also for their distribution along the tunnel boundary. On the other hand, both VLM-free method and VLM-fix method give bending moment diagrams which are significantly different from that of the 3D model (see Fig. 11).

For normal forces induced in the tunnel lining determined by the 2D deconfinement methods, the VLM-free method gives results which are in good agreement with the

**Fig. 10** Surface settlements (a) and lateral displacements (b) at a distance  $2L_S$  behind the shield tail and also section at the final state



3D model. On the other hand, the VLM-fix method gives the worst results.

In reality, the bending moment and the normal forces must be taken into account together to evaluate the lining loading. When considering only structural forces induced in the tunnel lining and using the error function presented in Eq. (2), the CCM method gives the better agreement with the 3D model. On the other hand, the worst results are obtained with the VLM-free method. The error function values obtained with the VLM-free method, the VLM-fix method and the CCM method are, respectively, equal to 0.164, 0.147 and 0.097.

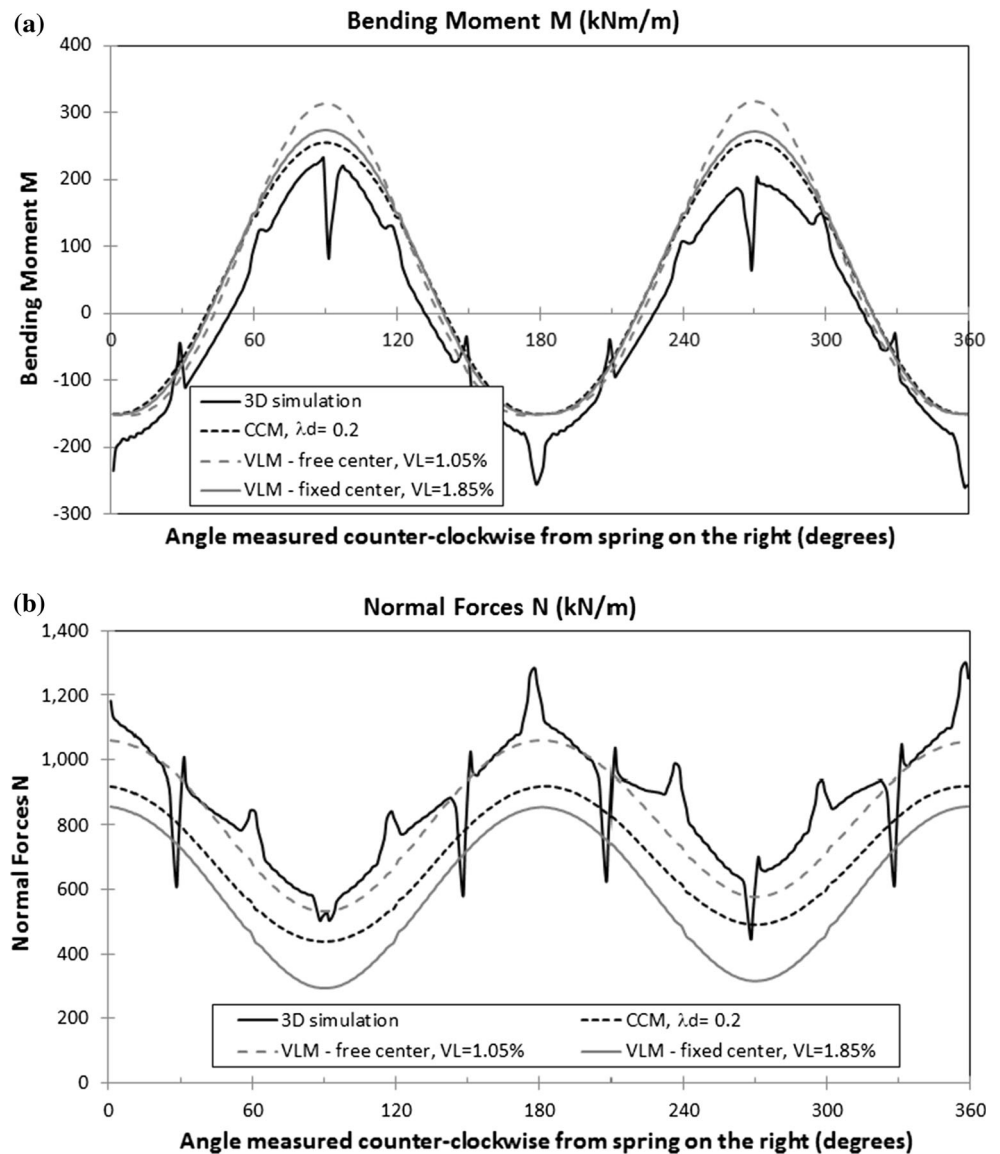
The CCM method can be used efficiently when considering only the lining internal forces. The VLM-free method is appropriate to use in the case of paying attention to both settlement trough and lateral movement of the soil surrounding the tunnel. Each deconfinement method, i.e., CCM method and VLM-free method, has a different efficiency for the estimation of structural forces and soil movements.

When both soil movements and tunnel lining internal forces are taken into account (scenario 5), the 2D better method is the VLM-free method, followed by the CCM method. The worst 2D simulation is obtained with the VLM-fix method. Indeed, the error function values obtained with the VLM-free method, the CCM method and the VLM-fix method are, respectively, equal to 0.468, 0.514 and 0.739. In other words, the VLM-fix method representing a uniform closure of the tunnel boundaries after excavation should not be used in 2D models. This observation is also similar as the one of Tamagnini et al. (2005).

## Conclusions

This paper presents a numerical investigation in which significant influences of the deconfinement methods on tunnel behavior are observed. On the basis of comparison

**Fig. 11** Bending moments (a) and normal forces (b) induced in the tunnel lining at the final state



with the 3D numerical model, the better 2D deconfinement method was estimated using the error function.

Depending on what is the most important parameter need to be monitored, different 2D deconfinement method should be adopted:

- When considering only the vertical settlement develop on the soil surface, the CCM method should be adopted;
- When considering the vertical settlement develop on the soil surface and the lateral movement of the soil surrounding the tunnel, the VLM-free method should be chosen;
- When considering only the structural forces induced in the tunnel, the CCM method should be chosen;

- When considering overall the behavior of the soil and tunnel lining, the VLM-free method is the better one.

In the case of paying attention to only soil movements, the optimum value of volume loss ratio (VL) or deconfinement factor ( $\lambda_d$ ) adopted in the VLM and CCM methods, respectively, using different optimization scenarios is more or less similar. It means that one of the optimization scenarios from 1 to 4 can be used to estimate the optimum relaxation parameter (VL or  $\lambda_d$ ) applied to 2D simulations without significant differences to the final results.

3D calculations were considered as the reference in this study due to the lack of monitoring on the Hanoi metro project which is under preparation for construction.

Experimental studies will be necessary in the future to validate the numerical results obtained in this study.

**Acknowledgements** This research is funded by Vietnam National Foundation for Science and Technology Development (NAFOSTED) under grant number 105.08-2015.14.

## References

- Addenbrooke TI, Potts DM, Puzrin AM (1997) The influence of pre-failure soil stiffness on the numerical analysis of tunnel construction. *Geotechnique* 47(3):693–712
- Arnau O, Molins C (2012) Three dimensional structural response of segmental tunnel linings. *Eng Struct* 44:210–221
- Callari C, Casini S (2005) Tunnels in saturated elasto-plastic soils: three-dimensional validation of a plane simulation procedure. In: Frémond M, Maceri F (eds) *Mechanical modeling and computational issues in civil engineering*. Springer, Berlin, Heidelberg, pp 143–164
- Cattani E, Miriano C, Boco L, Tamagnini C (2016) Time dependent ground movements induced by shield tunnelling in soft clay: a parametric study. *Acta Geotech* 11(6):1385–1399. doi:10.1007/s11440-016-0452-x
- Do NA, Dias D, Oreste PP, Djeran-Maigre I (2013) 2D numerical investigation of segmental tunnel lining behavior. *Tunnel Undergr Space Technol* 37:115–127
- Do NA, Dias D, Oreste PP, Djeran-Maigre I (2014a) 2D tunnel numerical investigation: the influence of the deconfinement method on tunnel behaviour. *Geotech Geol Eng* 32(1):43–58
- Do NA, Dias D, Oreste PP, Djeran-Maigre I (2014b) Two-dimensional numerical investigation of twin tunnel interaction. *Geomech Eng* 6(3):263–275
- Do NA, Dias D, Oreste PP, Djeran-Maigre I (2014c) Three-dimensional numerical simulation of a mechanized twin tunnels in soft soil. *Tunn Undergr Space Technol* 42:40–51
- Do NA, Dias D, Oreste PP (2014d) 3D numerical investigation on the interaction between mechanized twin tunnels in soft soil. *Environ Earth Sci* 73(5):2101–2113
- Do NA, Dias D, Oreste PP (2014e) Three-dimensional numerical simulation of mechanized twin stacked tunnels in soft soil. *J Zhejiang Univ Sci A* 15(11):896–913
- Do NA, Dias D, Oreste PP, Djeran-Maigre I (2014f) Three-dimensional numerical simulation for mechanized tunnelling in soft soil: the influence of the joint pattern. *Acta Geotech* 9(4):673–694
- Do NA, Dias D, Oreste PP (2015) 3D Numerical investigation of mechanized twin tunnels in soft soil—influence of lagging distance between two tunnel faces. *Eng Struct* 109:117–125. doi:10.1016/j.engstruct.2015.11.053
- Hanoi Metropolitan Railway Management Board (MRB) (2012) Hanoi pilot light metro line 3, section Nhon-Hanoi Railway Station-Technical design of underground section-line and stations. Package No.: HPLMLP/CP-03
- Hejazi Y, Dias D, Kastner R (2008) Impact of constitutive models on the numerical analysis of underground constructions. *Acta Geotech* 3:251–258
- Itasca Consulting Group, Inc. (2009) *FLAC fast lagrangian analysis of continua. Version 4.0. User's manual*
- Janin JP, Dias D, Kastner R, Emeriault F, Le Bissonnais H, Guilloux A (2015) Numerical back-analysis of the southern Toulon tunnel measurements: a comparison of 3D and 2D approaches. *Eng Geol* 195:42–52
- Jenck O, Dias D (2004) Analyse tridimensionnelle en différences finies de l'interaction entre une structure en béton et le creusement d'un tunnel à faible profondeur. *Geotechnique* 8(54):519–528
- Karakus M (2007) Appraising the methods accounting for 3D tunnelling effects in 2D plane strain FE analysis. *Tunn Undergr Space Technol* 22:47–56
- Möller SC, Vermeer PA (2008) On numerical simulation of tunnel installation. *Tunnel Undergr Space Technol* 23:461–475
- Mollon G, Dias D, Soubra AH (2013) Probabilistic analyses of tunnelling-induced soil movements. *Acta Geotech* 8(2):181–199
- Muniz de Farias M, Júnior AHM, Pacheco de Assis A (2004) Displacement control in tunnels excavated by the NATM: 3-D numerical simulations. *Tunn Undergr Space Technol* 19(3):283–293
- Negro A, Queiroz BIP (2000) Prediction and performance of soft soil tunnels. In: *Geotechnical aspects of underground construction in soft soil*, Balkema, Tokyo, Japan, pp 409–418
- Panet M, Guenot A (1982) Analysis of convergence behind the face of a tunnel. In: *Proceedings of the international symposium, tunnelling*, pp 187–204
- Rowe RK, Lo KY, Kack KJ (1983) A method of estimating surface settlement above shallow tunnels constructed in soft soil. *Can Geotech J* 20:11–22
- Surarak C (2010) *Geotechnical aspects of the Bangkok MRT blue line project*. Ph.D. dissertation, Griffith University
- Svoboda T, Masin D (2009) Comparison of displacement field predicted by 2D and 3D finite element modeling of shallow NATM tunnels in clays. *Geotechnik* 34:115–126
- Svoboda G (1979) Finite element analysis of the New Austrian Tunnelling Method (NATM). In: *Proceedings of 3rd international conference on numerical methods in geomechanics, Aachen, vol 2*, p 581
- Tamagnini C, Miriano C, Sellari E, Cipollone N (2005) Two dimensional FE analysis of ground movements induced by shield tunnelling: the role of tunnel ovalization. *Riv Ital Geotech* 1:11–33
- Vermeer PA, Brinkgreve R (1993) *Plaxis version 5 manual*. A.A. Balkema, Rotterdam
- Wongsaraj J, Soga K, Mair R (2013) Tunnelling induced consolidation settlements in London clay. *Geotechnique* 63(13):1103–1115